Tropical Daytime Lower D-region Dependence on Sunspot Number

Neil R. Thomson and Craig J. Rodger

Physics Department, University of Otago, Dunedin, New Zealand

Mark A. Clilverd

British Antarctic Survey, Cambridge, UK

Abstract

Observed phases and amplitudes of VLF radio signals propagating on (near) tropical all-sea paths, both short, ~300 km, and long, ~10 Mm, are used to find daytime parameter changes for the lowest edge of the (D-region of the) Earth's ionosphere as the solar cycle advanced from a very low sunspot number of ~5 up to ~60, in the period 2009-2011. The VLF phases, relative to GPS 1-sec pulses, and amplitudes were measured ~100 km from the transmitter, where the direct ground wave is very dominant, ~300 km from the transmitter, near where the ionospherically reflected waves form a (modal) minimum with the ground wave, and ~10 Mm away where the lowest order waveguide mode is fully dominant. Most of the signals came from the 19.8 kHz, 1-MW transmitter, NWC, North West Cape, Australia, propagating ENE, mainly over the sea, to the vicinity of Karratha and Dampier on the NW coast of Australia and then on to Kauai, Hawaii, ~10.6 Mm from NWC. Observations from the 8.1-Mm path NPM (21.4 kHz, Hawaii) to Dunedin, NZ, are also used. The sunspot number increase from ~5 to ~60 was found to coincide with a decrease in the height, H', of the midday tropical ionosphere by 0.75 ±0.25 km (from $H' \approx 70.5$ km to $H' \approx 69.7$ km) while the sharpness, β increased by 0.025 ±0.01 km^{-1} (from $\beta \approx 0.47$ km^{-1} to $\beta \approx 0.49$ km^{-1}) where H' and β are the traditional height and sharpness parameters used by Wait and by the US Navy in their Earth-ionosphere VLF radio waveguide programs.

1. Introduction

The lower D-region (~50-75 km altitude) is the lowest edge of the Earth's ionosphere. The principal ionizing sources generating free electrons in this region are solar EUV radiation and galactic cosmic rays. Very Low Frequency (VLF) radio waves (~3-30 kHz) radiated from near the ground are reflected from both the lower D-region and the Earth's surface which together form the Earth-ionosphere wave guide. Observations of phase changes and attenuations along the paths of these VLF signals allow one of the best techniques available for measuring the height and sharpness of the ionization in lower D-region. Such electron number density profiles, particularly their latitudinal, diurnal, seasonal and solar cycle changes, are not readily measured by means other than VLF [e.g., *Thomson et al.*, 2011b].

Knowledge of the height and sharpness of the unperturbed lowest edge of the ionosphere is important because these parameters are used as baselines in many areas of current research, as well as for predicting radio propagation conditions. Energetic particle precipitation from the Earth's radiation belts due to both natural and man-made effects [e.g., *Gamble et al.*, 2008; *Clilverd et al.*, 2009] require accurate D-region baseline parameters in order to calculate the precipitating fluxes. VLF propagation in the Earth ionosphere waveguide is also used in many lightning studies [e.g., *Jacobson et al.*, 2010], especially for the World Wide Lightning Location Network, WWLLN [e.g., *Dowden et al.,* 2008; *Rodger et al.*, 2004, 2006]. Solar cycle-induced changes in the unperturbed ionosphere can introduce uncertainty in the estimates of radio propagation conditions, energetic particle fluxes, and lightning location/power unless they are accurately quantified. Quantification of solar cycle forcing variations of the chemistry of the D-region is also of use in order to constrain and improve ion and neutral chemical modeling [e.g., *Verronen et al.*, 2005].

VLF radio propagation in the Earth-ionosphere waveguide is modeled by computer programs (MODESRCH, ModeFinder, LWPC - Long Wave Propagation Capability) developed by the US Naval Ocean Systems Center (NOSC) [e.g. *Morfitt and Shellman,* 1976; *Ferguson and Snyder*, 1990].

Such modeling and comparisons with observations can be found in *Thomson et al.* [2011b] and references therein. These modeling programs can input any profile for electron density versus height for the lower D-region (and hence the upper bound of the waveguide) but, unfortunately there are then too many parameters. As in previous studies by ourselves, NOSC and others [e.g., *Thomson et al.*, 2011b], we model the D-region with a Wait ionosphere defined by just two parameters, the 'reflection height', H', in km, and the exponential sharpness factor, β, in km^{-1} [*Wait and Spies,* 1964]. Appropriate values of these two parameters are then input into ModeFinder or LWPC which then calculates the expected phase and amplitude changes along the path; these calculations, for various input values of H' and β, can then be compared with observations to find matches. For the short (~300 km) low-latitude path, NWC to Karratha, on the coast of N.W. Australia (~20º S geographic, ~30º S geomagnetic), *Thomson* [2010] used VLF observations plus ModeFinder to determine H' = 70.5 km and β = 0.47 km^{-1} near midday in October 2009, i.e. at solar minimum with the Sun near the zenith. *Thomson et al.* [2011b] used the same technique on the long, 10.6 Mm, path from NWC to Kauai, Hawaii, also in October 2009 at solar minimum, and found H' and β values consistent with the solar minimum values on the short NWC-Karratha path.

Here, we report the results of very similar measurements made in 2011 (mainly in October) when, due to the advancing solar cycle, the smoothed (12-month running mean) sunspot number had risen to ~60 from ~5 in October 2009. The observed phases and amplitudes are then compared with calculations using the ModeFinder and LWPC codes to determine the changes in H' and β at tropical latitudes caused by this rising solar activity.

2. VLF Measurement Techniques

2.1 The Portable VLF Loop Antenna and Receiver

The phases and amplitudes of the VLF signals were measured with a portable loop antenna with battery powered circuitry. The phase was measured (modulo half a cycle) relative to the 1-s pulses from a GPS receiver built in to the portable VLF circuitry. Details of the portable loop and its phase and amplitude measuring techniques are given in *Thomson* [2010].

2.2 The Fixed VLF Recorders

NWC and NPM, in common with other US Navy VLF transmitters, typically have very good phase and amplitude stability. However, they not uncommonly undergo occasional phase drifts or jumps especially coinciding with their weekly off-air maintenance periods. To check and allow for such phase drifts or jumps, two continuously operating fixed 'softPAL' receivers [*Dowden and Adams*, 2008] recorded both amplitude and GPS-referenced phase in Dunedin, NZ, where the signal to noise ratio for both transmitters is very good. (Further details can be found in *Thomson* [2010]).

3. VLF Measurements and Modeling Comparisons

3.1 The Paths

Figure 1 shows the locations of the NWC and NPM transmitters, the principal receiving locations and the paths which, as can be seen, are mainly over the sea.

3.2 NWC, Australia, Observations During October 2011

The measurement places, techniques and analysis used here are very similar to those used for October 2009 by *Thomson* [2010] where further details can be found. Figure 2 shows the phases and amplitudes of NWC at Dunedin, NZ (5.7 Mm away) recorded while the portable loop phase and amplitude measurements were being made in N.W. Australia during the 8 days 9-16 Oct 2011. Portable loop measurements were made in the Karratha/Dampier area on ~4.5 of these days and in the Onslow area (~3 hours drive from Karratha) on ~2.5 of these days (12-14 Oct 2011) while on the other day (10 Oct 2011) NWC was off-air for its routine weekly maintenance. In Figure 2 the Dunedin amplitude plot (in dB above an arbitrary level) shows a spread of only ~±0.4 dB, apart from occasional solar flares, e.g. near 06 UT on 12 Oct 2011. This stability of path is typical for the summer half of the year. The Dunedin phase plot (referenced to GPS 1-sec pulses) appears at first sight to be less reproducible from day to day; however, as has been shown previously [*Thomson*, 2010], these phase drifts are occurring at the transmitter, not on the NWC-Dunedin path, and can be readily allowed for in our overall NWC analysis by using this Dunedin phase plot.

Over 25 sets of portable loop phase and amplitude measurements of NWC signals were made at Onslow spread over the 3 days 12-14 Oct 2011. All the measurements were made within 3-4 hours of midday, mainly within 2 hours. Seven sites were used with ranges from the transmitter of ~93-100 km. As with the similar measurements taken in October 2009 [*Thomson*, 2010], all the measured phase delays were adjusted for the different ranges from the transmitter (1.0 μs per 300 m) to allow comparison of sites. The agreement between sites on each of the days was again very good (within a few tenths of 1 μs).

The amplitude of the NWC signal around Onslow is very high (~100 mV/m), higher than the portable loop receiver was initially designed for. As previously [*Thomson*, 2010], this was dealt with by reducing the gain at Onslow by replacing the two 39 Ω resistors usually used in series with the loop coil with two 2.0 kΩ resistors. The resulting gain change and phase shift was readily calculated (using the measured loop inductance) and confirmed in the field at Karratha (where the midday field strength is ~10 mV/m) by alternating the gains.

As can be found from Figure 2, the average NWC phase measured at Dunedin near midpath midday (i.e., midday at the path midpoint) for NWC-Dunedin (0100-0400 UT) for the three Onslow measurement days, 12-14 Oct 2011, was -90°. The corresponding average of the phase delays measured at Onslow (~100 km from NWC) with the portable loop system was 2.3 μs (relative to the loop system's GPS 1-s pulse after adjusting to the loop using 2 × 39 Ω from the measurements made using 2 × 2.0 kΩ - details in *Thomson* [2010]). These two phase values, -90° at Dunedin and 2.3 μs at Onslow, are used below with the corresponding phase values from Karratha and Dampier.

3.3 Observations at Karratha during October 2011 compared with Modeling

As in 2009 [*Thomson*, 2010], Karratha and Dampier (~300 km from NWC) are close to or slightly beyond a modal minimum from NWC on 19.8 kHz. Calculations and observations showed that near midday ~30 mV/m of ground wave (destructively) interferes with ~20 mV/m of ionospherically reflected waves to give ~10 mV/m of observed signal. This results in good sensitivity to the ionospheric reflections. In Karratha (20 km by road from Dampier), most of the measurements in 2009 were made on Millars Well Oval while in 2011 they were more conveniently made in the minipark beside Millars Well Oval (~100 m away). The effective difference between these two very nearby sites is small but the appropriate exact actual locations were used for the phase analyses in each of 2009 and 2011.

In 2011, portable loop measurements were made in the Millars Well minipark, Karratha, on the 5 days, 9, 11, 14, 15, and 16 October. (NWC was off-air for routine maintenance on 10 October.) As can be found from Figure 2, the average NWC phase measured at Dunedin near midpath midday (0100-0400 UT) for these 5 days, was -85°. The corresponding average of the phase delays measured in Karratha with the portable loop system was 18.7 μs (relative to the loop system's GPS 1-s pulse using the standard 2 x 39 Ω at the loop input).

Clearly the phase delays measured at Onslow (2.3 μs) and at Karratha (18.7 μs) need to be adjusted for the same phase at Dunedin (and hence at NWC) to find the phase delay (for the 19.8 kHz NWC signal) from Onslow to Karratha which is thus:

$$18.7 - 2.3 + [-85 - (-90)]/360/0.0198 = 17.1\ \mu\text{s}.$$

This delay is modulo a half a cycle of 19.8 kHz, due to both the nature of the MSK modulation used by NWC and to the portable phase meter being frequently powered off and on [*Thomson*, 2010].

This delay difference (between Onslow and Karratha) can be thought of as consisting of two parts: the free space part along the surface of the Earth and the ionospherically reflected part. Indeed VLF waveguide programs such as ModeFinder and LWPC output their phases relative to the free-space delay. Table 1 shows the locations of NWC and the principal sites used in each of Karratha and Onslow (using Google Earth and a portable GPS receiver). The distances in rows 2 & 3 were calculated using the Vincenty algorithm [*Vincenty*, 1975; www.ngs.noaa.gov/cgi-bin/Inv_Fwd/inverse2.prl; www.ga.gov.au/geodesy/datums/vincenty_inverse.jsp] and from these the free space delays were found using the exact speed of light, c = 299.792458 m/μs. The difference between the NWC-Karratha and NWC-Onslow free space delays, 666.6 μs, was then reduced by an integral number of half cycles: $666.6 - 26 \times 0.5/0.0198 = 10.0$ μs, to allow for the phase measuring half-cycle ambiguity. This free space delay was then subtracted from the observed delay giving the waveguide part of the delay difference between Onslow and Karratha, $17.1 - 10.0 = 7.1$ μs $\equiv 51^{o}$ which was then subtracted from the 45^{o} calculated by ModeFinder for the phase of NWC at Onslow giving -6^{o} for the 'observed' phase at Karratha shown in the top panel of Figure 3.

The average measured amplitudes of NWC at Millars Well, Karratha and at Onslow were 82.4 dB and 99.9 dB, respectively, above 1 μV/m. The ModeFinder calculated NWC amplitude at Onslow (for 1 MW radiated) was 100.2 dB above 1 μV/m, 0.3 dB greater than that observed, similar to that for the 2009 observations [*Thomson*, 2010]. The observed amplitude at Karratha for 1 MW radiated would thus have been $82.4 + 0.3 = 82.7$ dB above 1 μV/m; this is the 'observed' amplitude shown in the lower panel of Figure 3. Also shown in Figure 3 are ModeFinder calculations for B_y at Karratha (expressed as dB > 1 μV/m using $E_z = cB_y$) for NWC radiating 1 MW for appropriate values of H' and β over an all-sea path [*Thomson*, 2010]. It can be seen that the best fit to the observations is obtained with $H' = 69.65$ km and $\beta = 0.49$ km^{-1}, which is a reduction in H' of 0.75 km, and an increase in β of 0.02 km^{-1} compared with October 2009. These values were used (retrospectively) in ModeFinder to calculate the phase (45^{o}) and amplitude (100.2 dB) at Onslow above. As for the 2009 results [*Thomson*, 2010], this procedure required only one iteration because the ionospheric part of the signal at Onslow is only ~15% of the total at Onslow while it is effectively more than 100% at Karratha due to the modal minimum there.

As previously [*Thomson*, 2010, *Thomson et al.*, 2011ab] the VLF field measurements used a portable loop inherently measuring the horizontal magnetic field of the wave, B_y, (perpendicular to the direction of propagation, x). However, such field strengths, as here, are usually expressed in V/m by using $E_z = cB_y$ (where c is the speed of light). Both ModeFinder and LWPC codes give essentially the same results for E_z provided they are both set so as not to cut off high order modes or low electron densities [e.g., *Thomson*, 2010]. ModeFinder (outputting B_y) was convenient and appropriate [*Thomson*, 2010] for the short paths but LWPC had clear advantages for the long paths because it can allow automatically for solar zenith angle and geomagnetic dip and azimuth changing along the path.

3.4 Observations at Dampier during October 2011 compared with Modeling

As can be seen in Figure 1, the NWC-Dampier path is virtually all-sea. Measurements were made on 4 days, 9, 11, 15 and 16 Oct 2011, and at several sites, including Hampton Oval (~293 km from NWC, and chosen, as in 2009, as the principal site with its parameters given in Table 2) and Dampier Sports Oval which is ~1 km further from NWC than Hampton Oval. As for the Karratha observations, the phases measured at the two Dampier sites gave good agreement with each other when allowance was made for their different distances from NWC.

The Dampier measurements were processed in a very similar way to those for Karratha. From Figure 2, the average NWC phase measured at Dunedin, 0100-0400 UT, for the 4 Dampier measurement days, was -85°. The corresponding average of the phase delays measured at Dampier (Hampton Oval) with the portable loop system was 16.9 μs (relative to the loop system's GPS 1-s pulse using the standard 2 × 39 Ω at the loop input). Again, the phase delays measured at Onslow (2.3 μs) and at Dampier (16.9 μs) need to be adjusted to the same phase at Dunedin (and hence at NWC) to find the phase delay (for the 19.8 kHz NWC signal) from Onslow to Dampier which is thus:

$$16.9 - 2.3 + [-85 - (-90)]/360/0.0198 = 15.3 \ \mu\text{s}.$$

Again, this delay is modulo a half a cycle of 19.8 kHz and can be thought of as consisting of two parts: the free space part along the surface of the Earth and the ionospherically reflected part.

Table 2 is similar to Table 1 and shows the locations of NWC and the principal sites used in each of Dampier and Onslow. The difference between the NWC-Dampier and NWC-Onslow free-space delays, 641.7 μs, was then reduced by an integral number of half cycles: $641.7 - 25 \times 0.5/0.0198 = 10.4$ μs, to allow for the phase measuring half-cycle ambiguity. This free space delay was then subtracted from the observed delay giving the waveguide part of the delay difference between Onslow and Dampier, $15.3 - 10.4 = 4.9$ μs $\equiv 35^{o}$ which was then subtracted from the 45^{o} calculated by ModeFinder for the phase of NWC at Onslow giving 10° for the 'observed' phase at Dampier shown in the top panel of Figure 4.

The amplitudes measured at Hampton Oval were on average about 0.5 dB higher than those measured at Dampier Sports Oval - a smaller difference than for the 2009 amplitude measurements. For relative consistency between the 2011 measurements and the earlier 2009 measurements, a mean amplitude was again taken by weighting the two sites, Hampton:DampierSports, 2:1 [*Thomson*, 2010] resulting in 80.4 dB (in October 2011) which, after adding 0.3 dB to adjust NWC to 1 MW (as in the Karratha case), becomes 80.7 dB which is thus shown as the 'observed' amplitude solid line in Figure 4. As can be seen, from the two panels in Figure 4, the best fit at Dampier in October 2011 is very similar to that for Karratha in October 2011 (Figure 3), i.e. H' = 69.65 km and β = 0.49 km^{-1}, which, as for Karratha, is a reduction in H' of 0.75 km, and an increase in β of 0.02 km^{-1} compared with October 2009.

3.5 Karratha and Dampier Short Paths in August 2011

During 21-28 August 2011, observations were also made of NWC at Onslow, Karratha and Dampier, in a very similar way to those in October 2011 (sections 3.2, 3.3 and 3.4 above). For these August measurements (also near midday), the amplitude at Karratha was 82.1 dB and the 'observed' phase (determined with the aid of the ModeFinder phase at Onslow, as in section 3.2) was 9^{o}, resulting, from Figure 3, in H' = 70.3 km and β = 0.46 km^{-1}, while for Dampier the amplitude and observed phase were 79.8 dB and 28.5º respectively, resulting, from Figure 4, in H' = 70.3 km and β = 0.485 km^{-1}. The August averages are thus H' = 70.3 km and β = 0.47 km^{-1}, very close to the values found earlier in the solar cycle in October 2009, i.e. H' = 70.4 km and β = 0.47 km^{-1} [*Thomson*, 2010], but with the Sun, of course, nearer the zenith in October than in August (and with all paths treated as all-sea).

Table 3 compares the H' and β values found from the (midday) observations on the NWC-Karratha/Dampier short (300 km) paths. The solar minimum results, sunspot number ~5, for late June 2008 and October 2009, come from *Thomson* [2010] while the August and October 2011 results, for sunspot number ~60, are those reported above. The results shown in brackets for August 2008/2009, solar zenith angle ~33º, are an interpolation between solar minimum results from June (2008), solar zenith angle ~45º, and October (2009), solar zenith angle ~12º. The interpolations are approximate; they made use of the plots of H' and β versus the cosine of the solar zenith angle given by *Thomson* [1993]. The resulting August changes in H' and β from 2009 to 2011, 70.3 - 71.1 = - 0.8 km, and 0.47 - 0.445 = 0.025 km^{-1}, can be seen to be very similar to the observed October changes, 69.65 - 70.4 = - 0.75 km, and 0.49 - 0.47 = 0.02 km^{-1}, thus adding weight, though possibly not accuracy, to the measurements of the October (2009-2011, solar cycle) changes. Changes in the values of H' and β with solar cycle are also compared in Table 4, discussed later.

3.6 The 8.1 Mm path NPM to Dunedin: 2009 and 2011 Results Compared

Observations of phase and amplitude for the 21.4 kHz signals from NPM on Oahu, Hawaii, were also made in Dunedin (~8.1 Mm from NPM) and on Kauai (~130 km from NPM) 18-23 October 2011. These are compared with similar observations made in October 2009 and with LWPC modeling in Figure 5 [*Thomson et al.*, 2011b]. The other paths reported here, NWC-

Karratha/Dampier and NWC-Hawaii, are all contained within geomagnetic latitudes ~±30º and so can be thought of as (near) tropical. About 75% of the length of NPM-Dunedin path falls in this range; the remaining ~25% has geomagnetic latitudes ranging from 30º up to 53º at Dunedin. While the VLF propagation changes per Mm caused by the advancing solar cycle may be larger at the higher latitudes (due to the larger cosmic ray effects there), they will not be greatly larger and so their effect on the total path for NPM-Dunedin is unlikely be very significant.

As can be seen from Figure 5, during the period October 2009 to October 2011, our NPM observations and analysis show that H' has decreased by 0.65 km (from ~70.8 km down to ~70.15 km) while β has increased by 0.03 km^{-1} (from ~0.46 km^{-1} to ~0.49 km^{-1}), these values being averaged along the path in all cases. These changes are similar to those found above for the short paths in N.W. Australia, as can also be seen in Table 4 as discussed later. The NPM-Dunedin path has the advantage over the other paths reported on here that measurements were required at only 2 locations, Kauai and Dunedin, and the amplitudes measured at Dunedin could be averaged over a few weeks because of the continuously operating, calibrated, fixed recorders there.

3.7 The 10.6 Mm Tropical Path NWC to Kauai, Hawaii: 2009 and 2011 Results Compared

In 2011, measurements similar to those made in October 2009 [*Thomson et al.*, 2011b] were also made for the ~10.6 Mm path NWC to Kauai. Phases and amplitudes of NWC were measured with the portable loop system on the eastern side of the island of Kauai on five days, 18-23 Oct 2011. The prime receiving site there was the same site in Lydgate Park, as in 2009. The Onslow-Kauai free-space delay difference, modulo half a period of NWC's 19.8 kHz (0.5/0.0198 μs), was calculated, using the Vincenty algorithm and the exact speed of light as 19.5 μs (very slightly different from the 19.6 μs calculated for 2009 [*Thomson et al.*, 2011b] due to the very slightly different principal site in

Onslow). As mentioned previously in section 3.2, the phase of NWC was measured with the portable loop system at Onslow, 12-14 Oct 2011. Using a very similar procedure to that for the NWC-Karratha/Dampier paths (sections 3.3 and 3.4, i.e. via the Dunedin recordings), the portable loop measurements at Lydgate Park and Onslow gave the observed Onslow-Lydgate phase delay (modulo half a cycle of NWC) as 18.2 μs. Subtracting the calculated free-space delay of 19.5 μs (from above) from this observed 18.2 μs gave -1.3 μs ≡ -9° or, modulo half a cycle, 171°, for the waveguide-only part of the Onslow-Lydgate delay. Subtracting this 171° from the 134° calculated by LWPC (using H' = 69.7 km, β = 0.49 km^{-1}) for the phase of NWC at Onslow in October gave -37° which is thus shown as the "observed" phase of NWC at Lydgate Park in Figure 6 where it is compared with the LWPC-calculated NWC phases at Lydgate Park using suitable values of H' and β [*Thomson et al.*, 2011b].

The mean amplitude of the NWC signal measured at the Kauai sites (~10.6 Mm from NWC) at midpath midday (~01 UT) 18-23 October 2011 was 672 μV/m ≡ 56.6 dB above 1 μV/m. The "observed" amplitude for NWC is thus shown in Figure 6 as 56.6 + 0.3 dB = 56.9 dB (as would have been observed if NWC had been radiating a full 1 MW).

From Figure 6 it can be seen that H' = 69.9 km and β = 0.52 km^{-1} fit the observed phases and amplitudes for NWC-Kauai. This may be indicating that, along this long (10.6 Mm) equatorial path, during the rising solar cycle between October 2009 and October 2011, the average H' has reduced by 1.1 km while the average β has increased from 0.46 km^{-1} (Figure 6) to 0.52 km^{-1}. This could indicate a larger solar cycle change for this near equatorial path (average geomagnetic latitude ~|15º|) as compared with NWC-Karratha/Dampier (average geomagnetic latitude ~|30º|). This, in turn, could be due to the relatively small amounts of electrons from galactic cosmic rays at these low latitudes (which do not vary much with solar cycle) thus increasing the effects of increasing [NO] and Lyman-alpha due to the advancing solar cycle.

On the other hand, if the amplitude of NWC measured in Kauai over the few available days in October 2009, had been just 0.1-0.2 dB higher than that observed, then β would have been found as

0.47 km^{-1} in 2009 rather than 0.46 km^{-1}, in agreement with the alternative estimate derived from the 2009 short path measurements [*Thomson et al.*, 2011b]. Again if the few days of 2011 measurements of NWC at Kauai were anomalously/randomly high by ~0.5 dB, and were reduced by this 0.5 dB, then the average β would be found as 0.50 km^{-1} in 2011 and the changes in path-average H' and β between October 2009 and October 2011 would be 0.7 km and 0.03 km^{-1} respectively, essentially the same as for the other paths reported here. Alternatively, it could well be that due to the relatively high solar zenith angles (~±50º) at the ends of this 10.6 Mm path (longitude spread 87º), that the change in β near the ends of this path, between 2009 and 2011, is greater than for the lower solar zenith angles on the centre of this path or on the other paths here, all of which have lower solar zenith angles (even for NPM-Dunedin, the ends have only ~±35º). The galactic cosmic ray ionization does not, of course, vary with solar zenith angle, but the proportion of Lyman-alpha-NO ionization at solar zenith angles near ~±45º will be lower than for (the near dominance at) low solar zenith angles, and so the solar cycle changes in β near ~±45º solar zenith angles (where the magnitudes of the effects of Lyman-alpha and cosmic rays are more similar) could be more than for more overhead sun, which could thus result in measurably higher solar cycle changes in average β for longer paths such as NWC to Kauai.

4. Discussion, Summary and Conclusions

The changes in H' and β between October 2009 and October 2011 (from section 3 above), during which the smoothed (12-month running mean) sunspot number (SSN) increased from ~5 to ~60, are summarized in Table 4. The changes are each presented as the 2011 value minus the 2009 value; H' decreases and β increases as the sunspot number rises.

Two short paths were studied, NWC-Karratha and NWC-Dampier. Measurements at Onslow, close to the NWC transmitter, were used to effectively monitor the phases and amplitudes of NWC essentially right at the transmitter. The error in the observed phases at Karratha (300 km from NWC) was estimated from the scatter from day to day. This scatter showed a standard error (standard deviation in the mean) of about 3º of phase angle. At Onslow (where the signal is mainly the direct ground wave) the standard error was <~2º. Thus the standard error for each phase difference between Onslow (effectively a proxy for NWC) and Karratha was thus about 4º. In 2009 [*Thomson*, 2010], and in 2011 (Figure 3 above), the measured phase delays for NWC-Karratha were 9º and -6º respectively. Hence the change in the NWC-Karratha phase delay, 15º, will have an error of ~6º. The NWC-Dampier path gave very similar results. Although both the NWC-Dampier and NWC-Karratha paths share the Onslow measurements, the measurements taken at Karratha and Dampier are largely independent of each other and, since they represent the bulk of the error for each path, the results for the two paths have a significant degree of independence. For each of these two paths the errors in the differences in amplitudes measured between 2009 and 2011 are likely to be less than ~0.5 dB (because the equipment and measurement sites were very similar).

Two long paths were studied, NPM-Dunedin and NWC-Kauai. For the long path, NPM-Dunedin, with a fixed recorder at Dunedin, the error in the change in amplitude measured between October 2009 and October 2011 is likely to be less than ~0.3 dB; the error in the change in phase delay is ~2º.

For the long path, NWC-Kauai, the corresponding errors in the changes will be greater, ~0.5 dB and ~4$^{\text{o}}$ respectively.

Overall, for these essentially tropical paths, our results indicate that H' decreased by 0.75 ±0.25 km (from ~70.5 to 69.7 km) and β increased by 0.025 ±0.01 km^{-1} (from ~0.47 to ~0.49 km^{-1}) between October 2009 and October 2011, when the sunspot number increased from ~5 to ~60. (These values of 70.5 and 69.7 km for H' are 0.05-0.1 km higher than shown in Figures 3 and 4 with the all-sea conductivity calculations, to allow a small amount, as was done in *Thomson* [2010], for the average ground conductivity being a little lower than that of seawater; this, of course, makes no difference to the change in height.)

At these low latitudes, the intensity of galactic cosmic rays (which are the dominant daytime ionizing source below ~65 km altitude [e.g., *Banks and Kockarts*, 1973]) varies little with solar cycle [e.g. *Heaps*, 1978]. However both the concentration of Nitric Oxide, [NO], and the intensity of solar Lyman-alpha radiation, which together are the dominant source of electrons above altitudes of ~65 km in the lower D-region, do increase in the rising part of the solar cycle and so are likely to be the primary causes of the lowering of the ionospheric height parameter, H', and the increases in the ionospheric sharpness parameter, β. For the Wait [*Wait and Spies*, 1964] D-region model used by NOSC in the ModeFinder and LWPC codes, the electron number density, $N_e(z)$, as a function of height, z, is given by [e.g. *Thomson*, 1993]:

$$N_e(z) = 1.43 \times 10^{13} \exp\,(-0.15H') \times \exp\,[(\beta - 0.15)(z - H')].$$

Hence the ratio of the electron number density at height z = 70 km for our SSN=60 case to that for our SSN=5 case is about 1.4, i.e., our VLF results here are indicating the (near) tropical electron number density, N_e, at heights ~70 km, has increased by about 40%, while the sunspot number increased from 5 to 60 during the rising part of the solar cycle from October 2009 to October 2011.

If the dominant electron loss process at these heights (~70 km) were proportional to N_e (e.g., controlled by attachment to neutral oxygen), then this would represent an increase of about 40% in the rate of Lyman-alpha ionizing NO; on the other hand, if the dominant electron loss process were proportional to N_e^2 (due to the electrons recombining directly with the positive ions), then this would represent an increase of a factor of ~2 in the rate of Lyman-alpha ionizing NO. The chemistry of the D-region is not well-understood. Reality is probably somewhere in between these two values. A reasonable estimate would seem to be to take the increase in ionization rate as ~65 %. *Woods et al.* [2000] have shown that the solar Lyman-alpha intensity increases on average during a solar cycle by a factor of about 1.5 from solar minimum to solar maximum. The increase in smoothed sunspot number here (from 5 to 60) is about half that in the solar cycles considered by *Woods et al.* [2000]; so, from their results, the increase in Lyman-alpha intensity during our study period (October 2009 to October 2011) would be ~25%. The difference between the observed ionization rate increase of ~65% and the Lyman-alpha increase of ~25% is very likely due to the number density of NO increasing by ~33%. This [NO] increase near 70 km altitude is likely due to diffusion down from the increased rate of production of NO at heights above ~100 km caused by increased solar soft X-rays accompanying the rise in the solar cycle [*Barth et al.*, 2003].

Clearly it would be desirable to repeat these measurements at solar maximum or when the smoothed sunspot number is appreciably higher than studied here. The dependence of the lower D-region on smoothed sunspot number is a topic that warrants further study.

Acknowledgements

The authors are very grateful to their colleague, David Hardisty, for his design, development and construction of the VLF phase meter. Thanks also to http://rimmer/ngdc.noaa.gov of NGDC, NOAA, US Dept. of Commerce, for the digital coastal outline and to english.freemap.jp for their free outline map of Australia, both used in Figure 1.

References

Banks, P. M., and G. Kockarts (1973), Aeronomy, Academic, New York.

Barth, C. A., K. D. Mankoff, S. M. Bailey, and S. C. Solomon (2003), Global observations of nitric oxide in the thermosphere, *J. Geophys. Res.,108*(A1), 1027, doi:10.1029/2002JA009458.

Dowden, R.L. and C.D.D. Adams (2008), SoftPAL, Proceedings of the 3rd VERSIM Workshop, Tihany, Hungary, 15-20 September 2008.

Clilverd, M. A., C. J. Rodger, N. R. Thomson, J. B. Brundell, Th. Ulich, J. Lichtenberger, N. Cobbett, A. B. Collier, F. W. Menk, A. Seppälä, P. T. Verronen, and E. Turunen (2009), Remote sensing space weather events: the AARDDVARK network, Space Weather, 7, S04001, doi:10.1029/2008SW000412

Dowden, R.L., R.H. Holzworth, C J. Rodger, J. Lichtenberger, N.R. Thomson, A.R. Jacobson, E. Lay, J.B. Brundell, T.J. Lyons, S.O'Keefe, Z. Kawasaki, C. Price, V. Prior, P. Ortéga, J. Weinman, Y. Mikhailov, R. Woodman, X. Qie, G. Burns, A. Collier, O. Pinto Junior, R. Diaz, C. Adamo, E.R. Williams, S. Kumar, G.B. Raga, J.M. Rosado, E.E. Avila, M.A. Clilverd, T. Ulich, P. Gorham, T. J. G. Shanahan, T. Osipowicz, G. Cook, and Y. Zhao (2008), World-Wide Lightning Location Using VLF Propagation in the Earth-Ionosphere Waveguide, *IEEE Antennas and Propagation Mag.*, 50(5), 40-60.

Ferguson, J. A. and F. P. Snyder (1990), Computer programs for assessment of long wavelength radio communications, version 1.0: full FORTRAN code user's guide, *Naval Ocean Systems Center Tech. Doc. 1773, DTIC AD-B144 839*, Def. Tech. Inf. Cent., Alexandria, Va.

Gamble, R. J., C. J. Rodger, M. A. Clilverd, J. A. Sauvaud, N. R. Thomson, S. L. Stewart, R. J. McCormick, M. Parrot, and J.-J. Berthelier (2008), Radiation belt electron precipitation by manmade VLF transmissions, J. Geophys. Res., 113, A10211, doi: 10.1029/2008JA013369.

Heaps, M.G. (1978), Parameterization of the cosmic ray ion-pair production rate above 18 km. *Planet. Space Sci.*, 26, 513-517.

Jacobson, A.R., Shao, X-M., Holzworth R. (2010), Full-wave reflection of lightning long-wave radio pulses from the ionospheric D region: Comparison with midday observations of broadband lightning signals. *J. Geophys. Res*., 115, A00E27, 12 PP., doi:10.1029/2009JA014540.

Morfitt, D. G. and C. H. Shellman (1976), MODESRCH, an improved computer program for obtaining ELF/VLF/LF mode constants in an Earth-Ionosphere Waveguide. *Naval Electr. Lab. Cent. Interim Rep. 77T, NTIS Accession ADA032573*, Natl. Tech. Inf. Serv., Springfield, VA.

Rodger, C.J., Brundell J.B., Dowden, R.L. and Thomson, N.R. (2004), Location accuracy of long distance VLF lightning location network. *Annales Geophysicae* 22(3):747-758.

Rodger, C J, S W Werner, J B Brundell, N R Thomson, E H Lay, R H Holzworth, and R L Dowden (2006), Detection efficiency of the VLF World-Wide Lightning Location Network (WWLLN): Initial case study, Annales Geophys., 24, 3197-3214.

Thomson, N. R. (1993), Experimental daytime VLF ionospheric parameters, *J. Atmos. Terr. Phys., 55*, 173-184.

Thomson, N.R. (2010), Daytime tropical D-region parameters from short path VLF phase and amplitude, *J. Geophys. Res.*, *115*, A09313, doi:10.1029/2010JA015355.

Thomson, N.R., M. A. Clilverd and C. J. Rodger (2011a), Daytime midlatitude D-region parameters at solar minimum from short-path VLF phase and amplitude, *J. Geophys. Res.*, *116*, A03310, doi:10.1029/2010JA016248.

Thomson, N.R., C. J. Rodger and M. A. Clilverd (2011b), Daytime D-region parameters from long-path VLF phase and amplitude, *J. Geophys. Res.*, *116*, A11305, doi:10.1029/2011JA016910.

Verronen, P. T., Seppälä, A., Clilverd, M. A., Rodger, C. J., Kyrölä, E., Enell, C-F., Ulich, Th. (2005), and Turunen, E., Diurnal variation of ozone depletion during the October-November 2003 solar proton event, *J. Geophys. Res.*, 110(A9), doi:10.1029/2004JA010932.

Vincenty, T. (1975), Direct and inverse solutions of geodesics on the ellipsoid with application of nested equations, *Survey Review*, *22(*176), 88-93.
Wait, J.R., Spies, K.P., (1964), Characteristics of the Earth-ionosphere waveguide for VLF radio waves. *NBS Tech. Note 300*, Natl..Bur. of Stand., Boulder, CO.
Woods, T.N., Tobiska, W.K., Rottman, G.J., Worden, J.R., Improved solar Lyman alpha irradiance modeling from 1947 through 1999 based on UARS observations, *J. Geophys. Res.*, 105, A12, 27195-27215, 2000.

Figure Captions

Figure 1. The NWC and NPM transmitter sites (red diamonds), the receiver sites (blue circles) and the paths used for the VLF phase and amplitude measurements to find the D-region electron density parameters.

Figure 2. NWC phases and amplitudes recorded at Dunedin, NZ, 5.7 Mm away, during the times when the October 2011 measurements were being made in N.W. Australia.

Figure 3. NWC, received at Millars Well mini-park, Karratha, Western Australia. Comparisons of modeling (for an all-sea path) with observed midday phases and amplitudes in October 2009 and October 2011.

Figure 4. NWC, received at Hampton Oval, Dampier, Western Australia. Comparisons of modeling (for an all-sea path) with observed midday phases and amplitudes in October 2009 and October 2011.

Figure 5. NPM, Hawaii received at Dunedin, NZ. The observed midday phases and amplitudes are compared with modeling using E_z from LWPC.

Figure 6. NWC received at Kauai, Hawaii. The observed midday phases and amplitudes are compared with modeling using E_z from LWPC.

Table 1. Calculated Onslow-Karratha Free-Space Delay Differences[a]

Calculated Phases (μs)	Latitude (deg)	Longitude (deg E.)	Dist. (km)	Delay (μs)
NWC	-21.8163	114.1656		
Karratha (Millars Well)	-20.7408	116.8194	300.03	1000.8
Onslow	-21.6388	115.1153	100.20	334.2
Δf: Karratha – Onslow			199.83	666.6
Δf: modulo half a cycle				10.0
Δo: observed				17.1
W/guide delay (Δo – Δf)				7.1

[a]Rows 1–4 show the locations with calculated distances and free space delays for NWC-Karratha, NWC-Onslow and Onslow-Karratha. Row 5 then shows the Onslow-Karratha free-space delay difference modulo half a cycle of 19.8 kHz. This difference is then subtracted from the 17.1 μs observed delay (row 6), to give the waveguide only part of the delay as 7.1 μs (bottom row) which is equivalent to 51°. This observed 51° is then subtracted from the 45° calculated by ModeFinder for Onslow giving 45° -51° = -6° shown in Figure 3 as the 'observed' NWC phase at Karratha.

Table 2. Calculated Onslow-Dampier Free-Space Delay Differences[a]

Calculated Phases (μs)	Latitude (deg)	Longitude (deg E.)	Dist. (km)	Delay (μs)
NWC	-21.8163	114.1656		
Dampier (Hampton Oval)	-20.6666	116.7035	292.57	975.9
Onslow	-21.6388	115.1153	100.20	334.2
Δf: Dampier – Onslow			192.37	641.7
Δf: modulo half a cycle				10.4
Δo: observed				15.3
W/guide delay (Δo – Δf)				4.9

[a]Rows 1–4 show the locations with calculated distances and free space delays for NWC-Dampier, NWC-Onslow and Onslow-Dampier. Row 5 then shows the Onslow-Dampier free-space delay difference modulo half a cycle of 19.8 kHz. This difference is then subtracted from the 15.3 μs observed delay (row 6), to give the waveguide only part of the delay as 4.9 μs (bottom row) which is equivalent to 35°. This observed 35° is then subtracted from the 45° calculated by ModeFinder for Onslow giving 45° -35° = 10° shown in Figure 4 as the 'observed' NWC phase at Dampier.

Table 3. Comparison of Measured Short-Path H' and β by Season and Solar Cycle[a]

Month	2008/09 H' (km)	2008/09 β (km^{-1})	2011 H' (km)	2011 β (km^{-1})
October	70.4	0.47	69.65	0.49
August	(71.1)*	(0.445)*	70.3	0.47
June	72.1	0.405		

[a]The sunspot number in 2008-2009 was ~5, while in October 2011, it was ~60. The path was NWC to Karratha in N.W. Australia (~300 km), so that June is in winter with a solar zenith angle ~45º, and October is in spring with the Sun only ~12º from the zenith. (*See text for discussion of the interpolation.)

Table 4. Comparison of Observed Changes in H' and β with Solar Cycle[a]

Path	Path Length (Mm)	$\Delta H'$ (km)	$\Delta\beta$ (km^{-1})
NWC-Karratha	0.3	- 0.75	0.02
NWC-Dampier	0.3	- 0.75	0.02
NPM-Dunedin	8.1	- 0.65	0.03
NWC-Hawaii	10.6	- 1.1*	0.06*

[a]The changes are the October 2011 value minus the corresponding value in October 2009. The sunspot number in 2009 was ~5, while in October 2011, it was ~60. (*See text for discussion.)

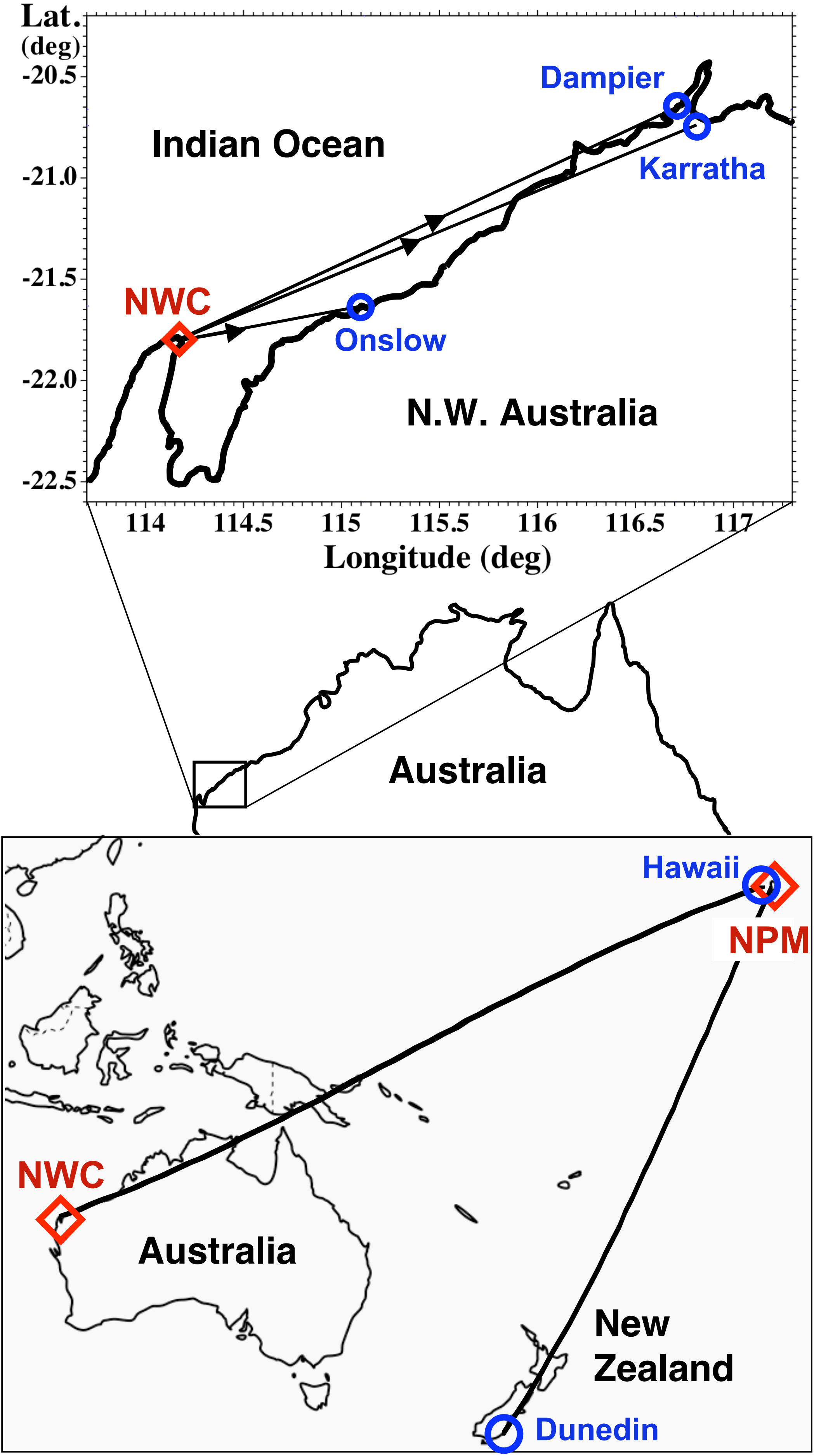
Lat.
(deg)
-20.5
-21.0
-21.5
-22.0
-22.5
Indian Ocean
Dampier
Karratha
NWC
Onslow
N.W. Australia
114
114.5
115
115.5
116
116.5
117
Longitude (deg)
Australia
Hawaii
NPM
NWC
Australia
New
Zealand
Dunedin

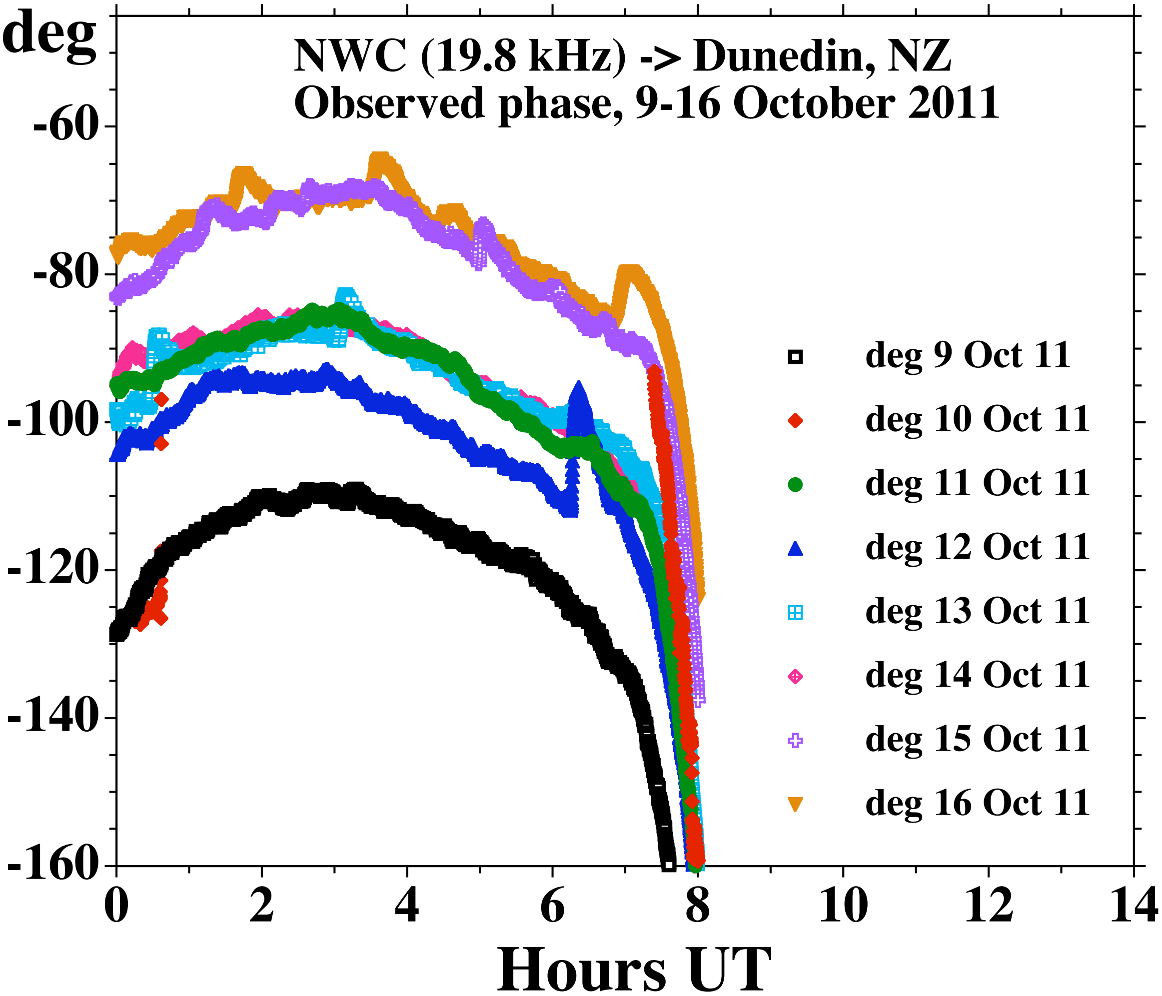
deg
NWC (19.8 kHz) -> Dunedin, NZ
Observed phase, 9-16 October 2011
-60
-80
-100
-120
-140
-160
deg 9 Oct 11
deg 10 Oct 11
deg 11 Oct 11
deg 12 Oct 11
deg 13 Oct 11
deg 14 Oct 11
deg 15 Oct 11
deg 16 Oct 11
0
2
4
6
8
10
12
14
Hours UT

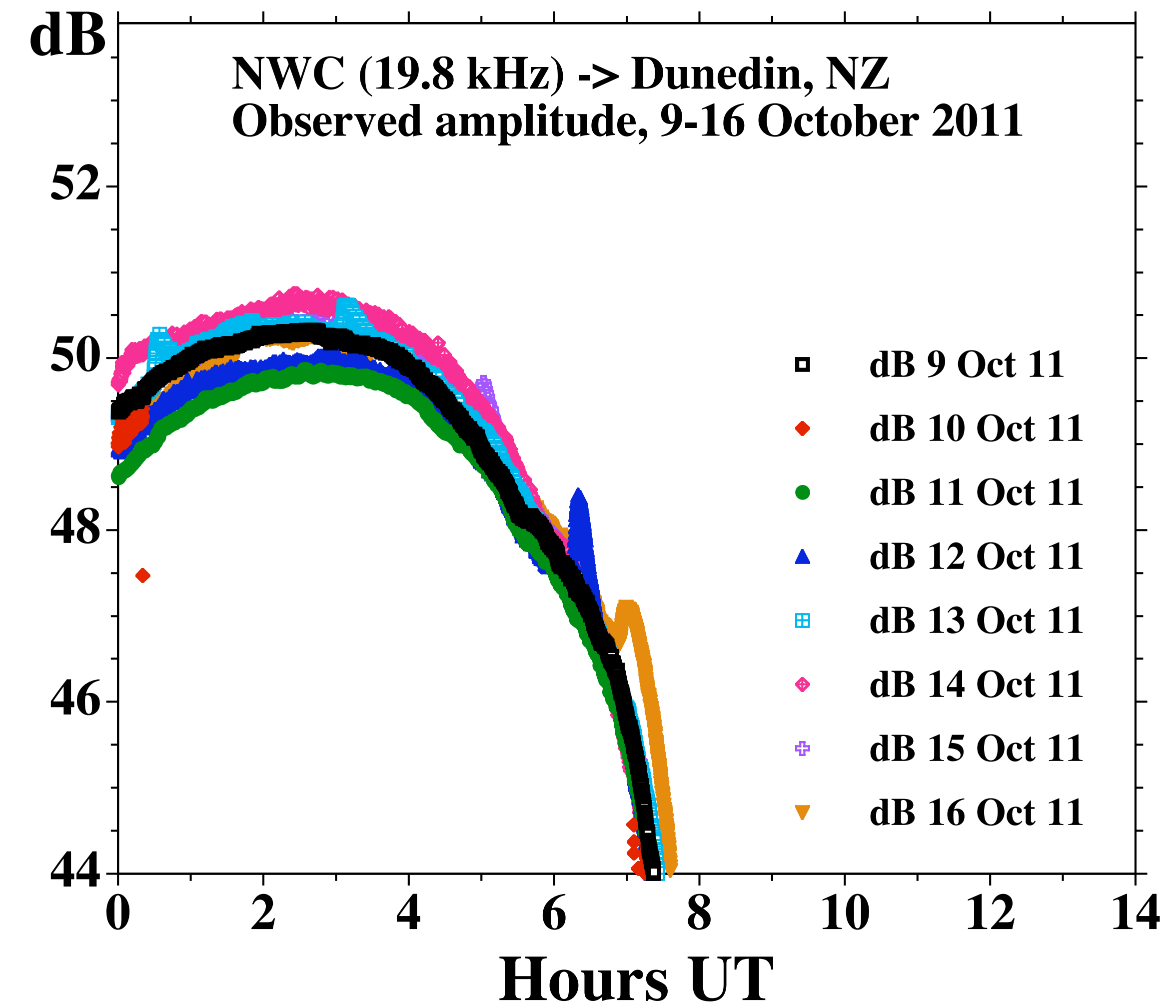
dB
NWC (19.8 kHz) -> Dunedin, NZ
Observed amplitude, 9-16 October 2011
52
50
48
46
44
dB 9 Oct 11
dB 10 Oct 11
dB 11 Oct 11
dB 12 Oct 11
dB 13 Oct 11
dB 14 Oct 11
dB 15 Oct 11
dB 16 Oct 11
0
2
4
6
8
10
12
14
Hours UT

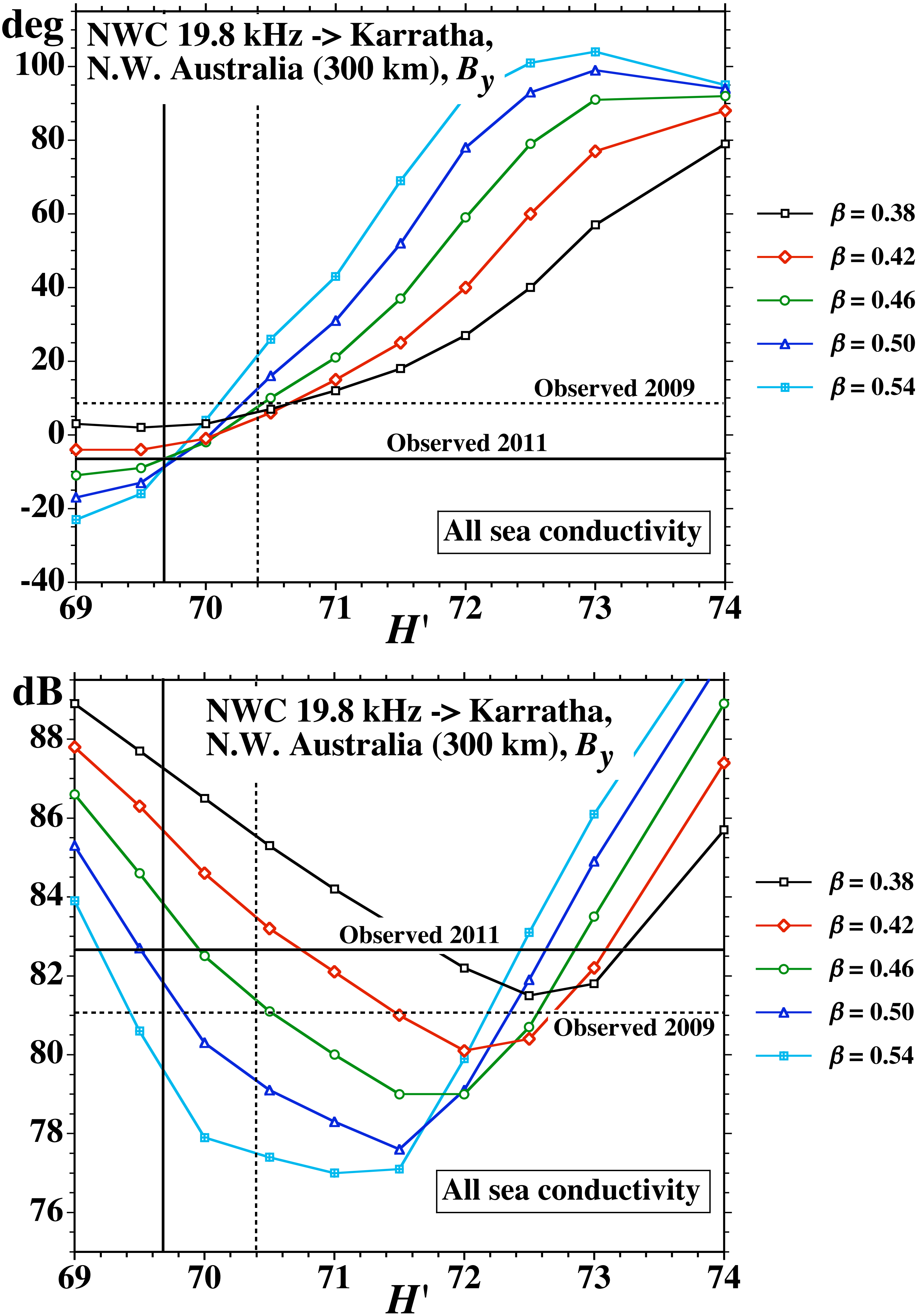

deg
NWC 19.8 kHz -> Karratha,
N.W. Australia (300 km), B_y
Observed 2009
Observed 2011
All sea conductivity
$\beta = 0.38$
$\beta = 0.42$
$\beta = 0.46$
$\beta = 0.50$
$\beta = 0.54$
-40
-20
0
20
40
60
80
100
69
70
71
72
73
74
H'
dB
NWC 19.8 kHz -> Karratha,
N.W. Australia (300 km), B_y
Observed 2011
Observed 2009
All sea conductivity
$\beta = 0.38$
$\beta = 0.42$
$\beta = 0.46$
$\beta = 0.50$
$\beta = 0.54$
76
78
80
82
84
86
88
69
70
71
72
73
74
H'

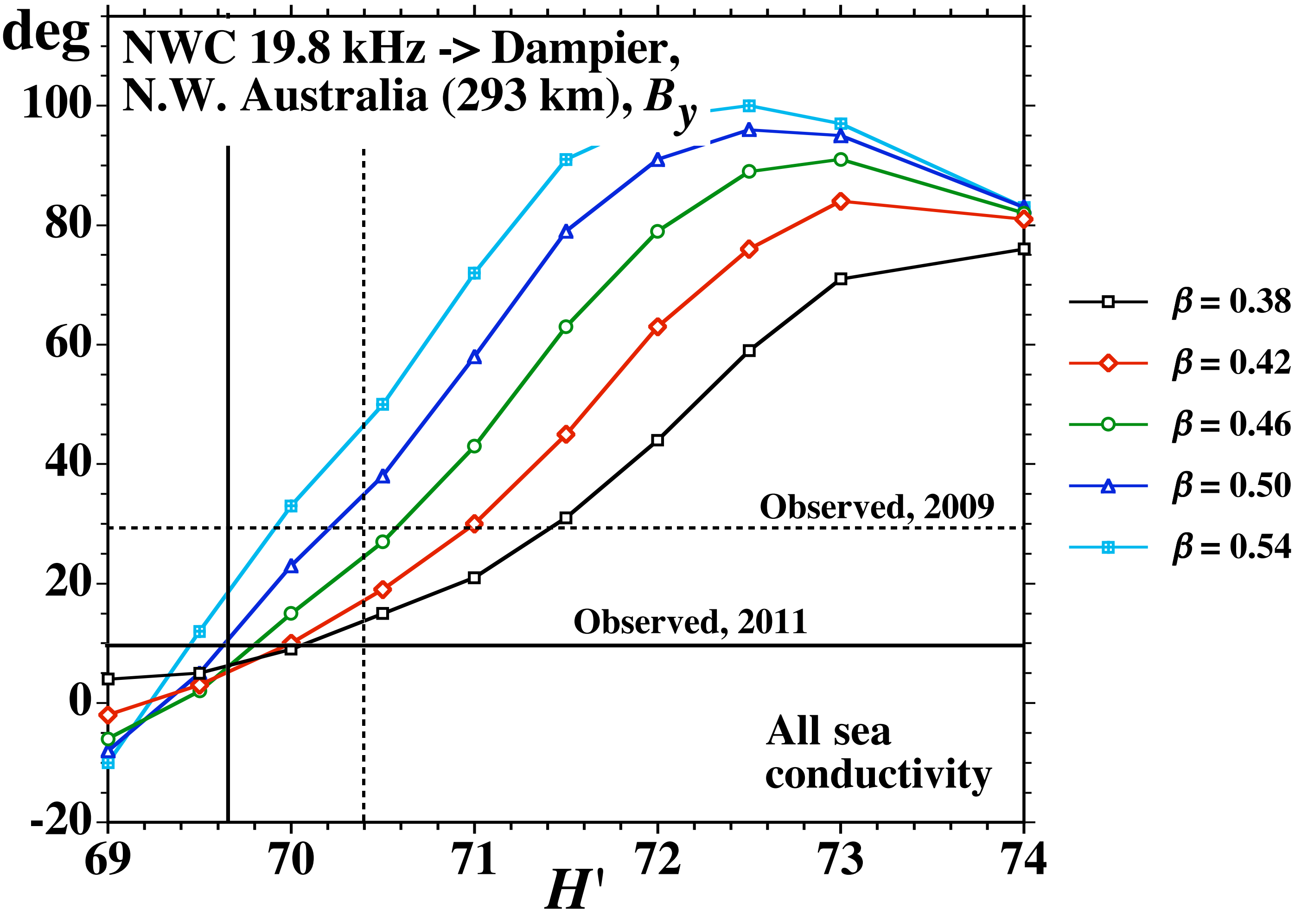

deg
NWC 19.8 kHz -> Dampier,
N.W. Australia (293 km), B_y
Observed, 2009
Observed, 2011
All sea
conductivity
H'
$\beta = 0.38$
$\beta = 0.42$
$\beta = 0.46$
$\beta = 0.50$
$\beta = 0.54$

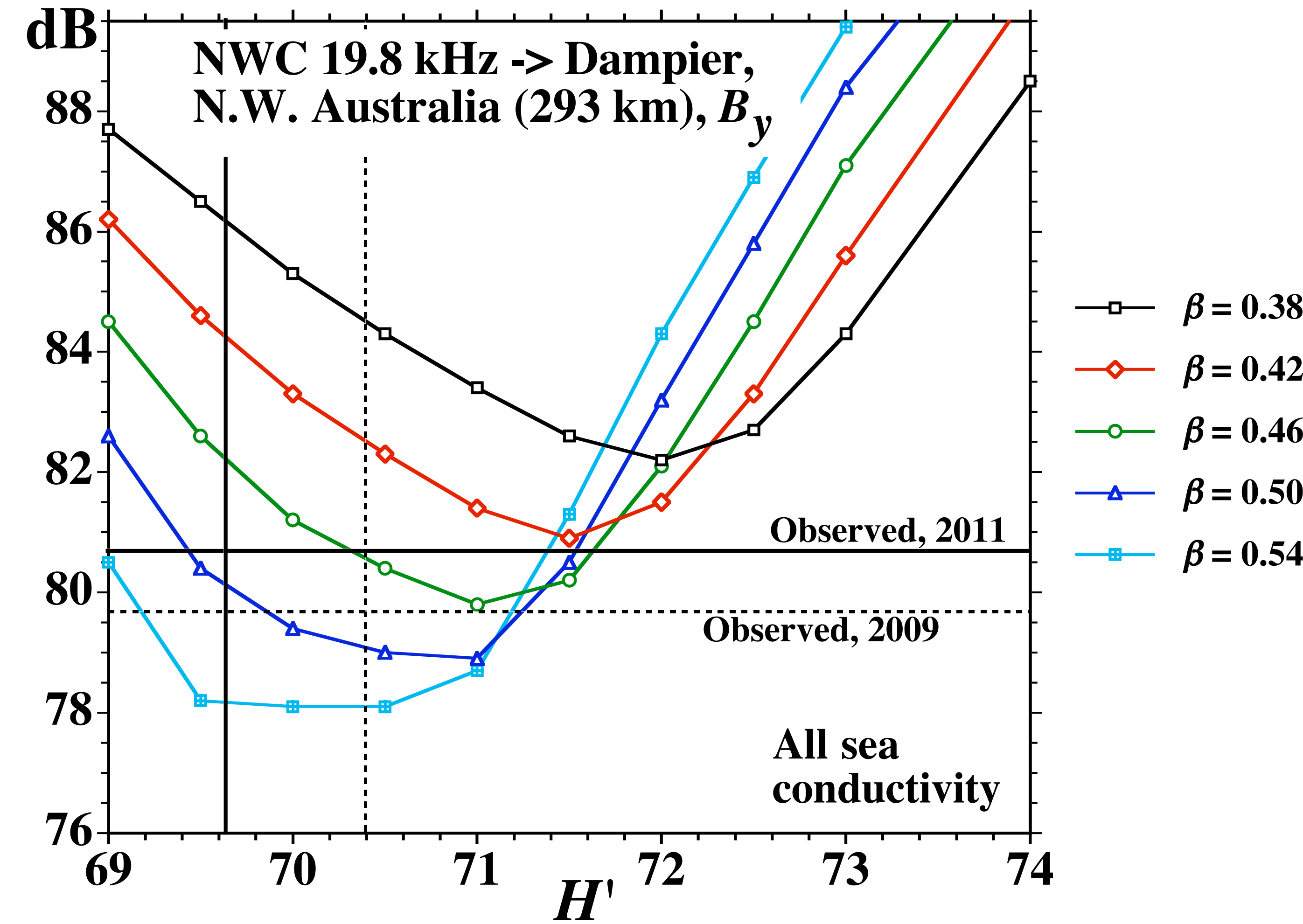

dB
NWC 19.8 kHz -> Dampier,
N.W. Australia (293 km), B_y
Observed, 2011
Observed, 2009
All sea
conductivity
H'
$\beta = 0.38$
$\beta = 0.42$
$\beta = 0.46$
$\beta = 0.50$
$\beta = 0.54$

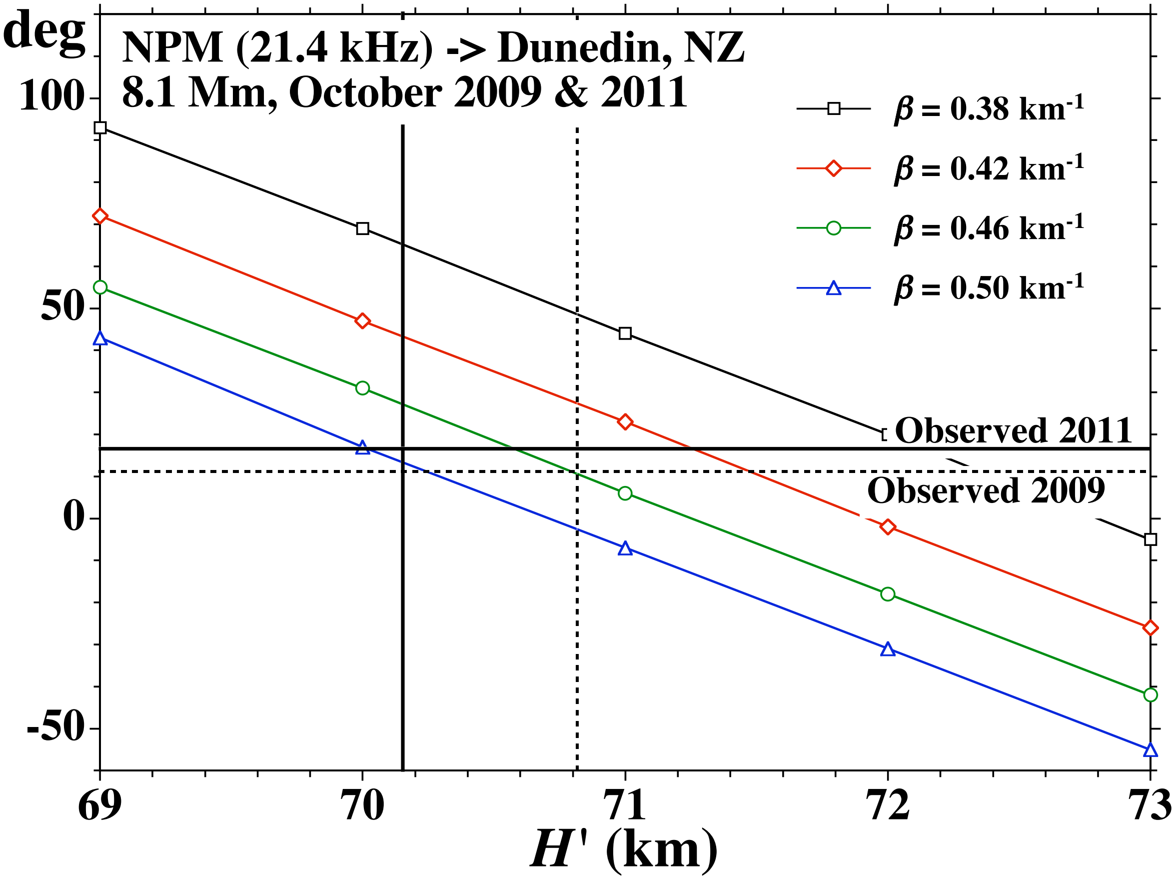

deg
NPM (21.4 kHz) -> Dunedin, NZ
8.1 Mm, October 2009 & 2011
β = 0.38 km-1
β = 0.42 km-1
β = 0.46 km-1
β = 0.50 km-1
Observed 2011
Observed 2009
100
50
0
-50
69
70
71
72
73
H' (km)

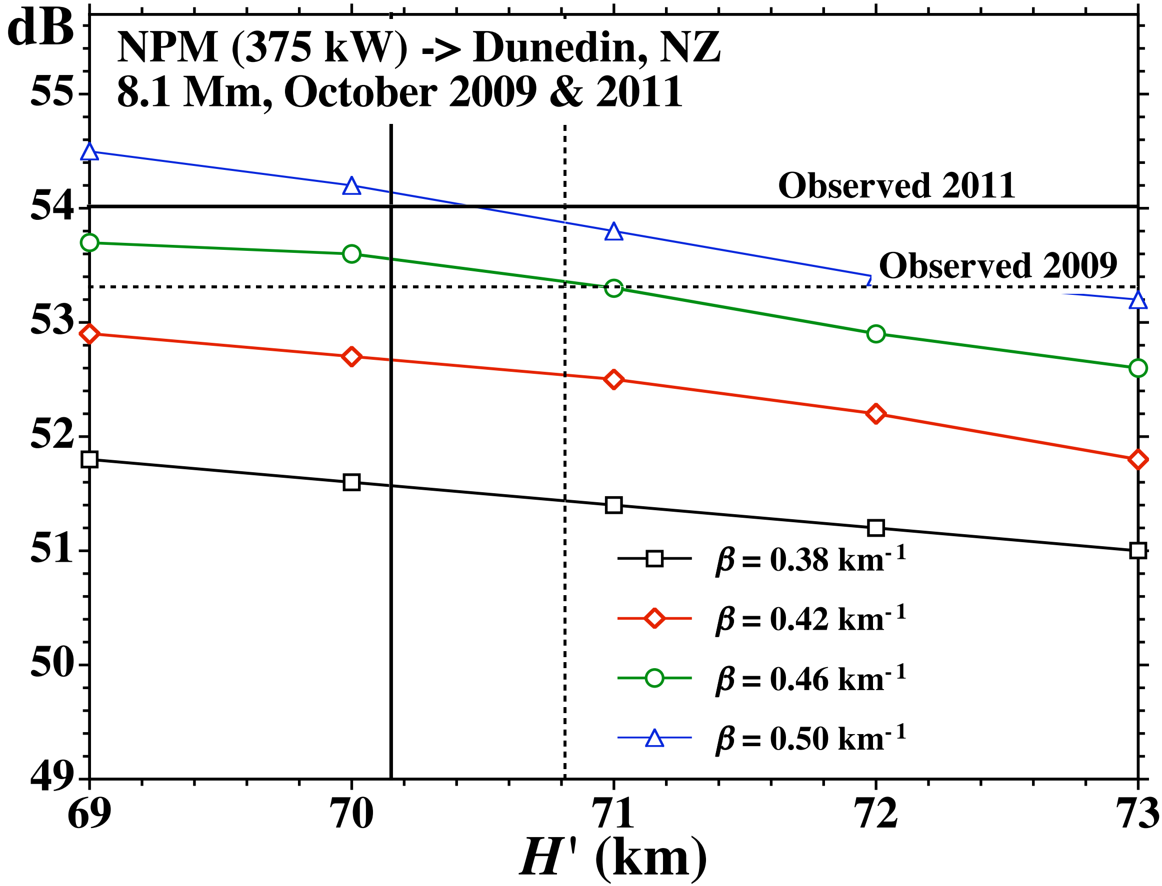

dB
NPM (375 kW) -> Dunedin, NZ
8.1 Mm, October 2009 & 2011
Observed 2011
Observed 2009
β = 0.38 km-1
β = 0.42 km-1
β = 0.46 km-1
β = 0.50 km-1
55
54
53
52
51
50
49
69
70
71
72
73
H' (km)

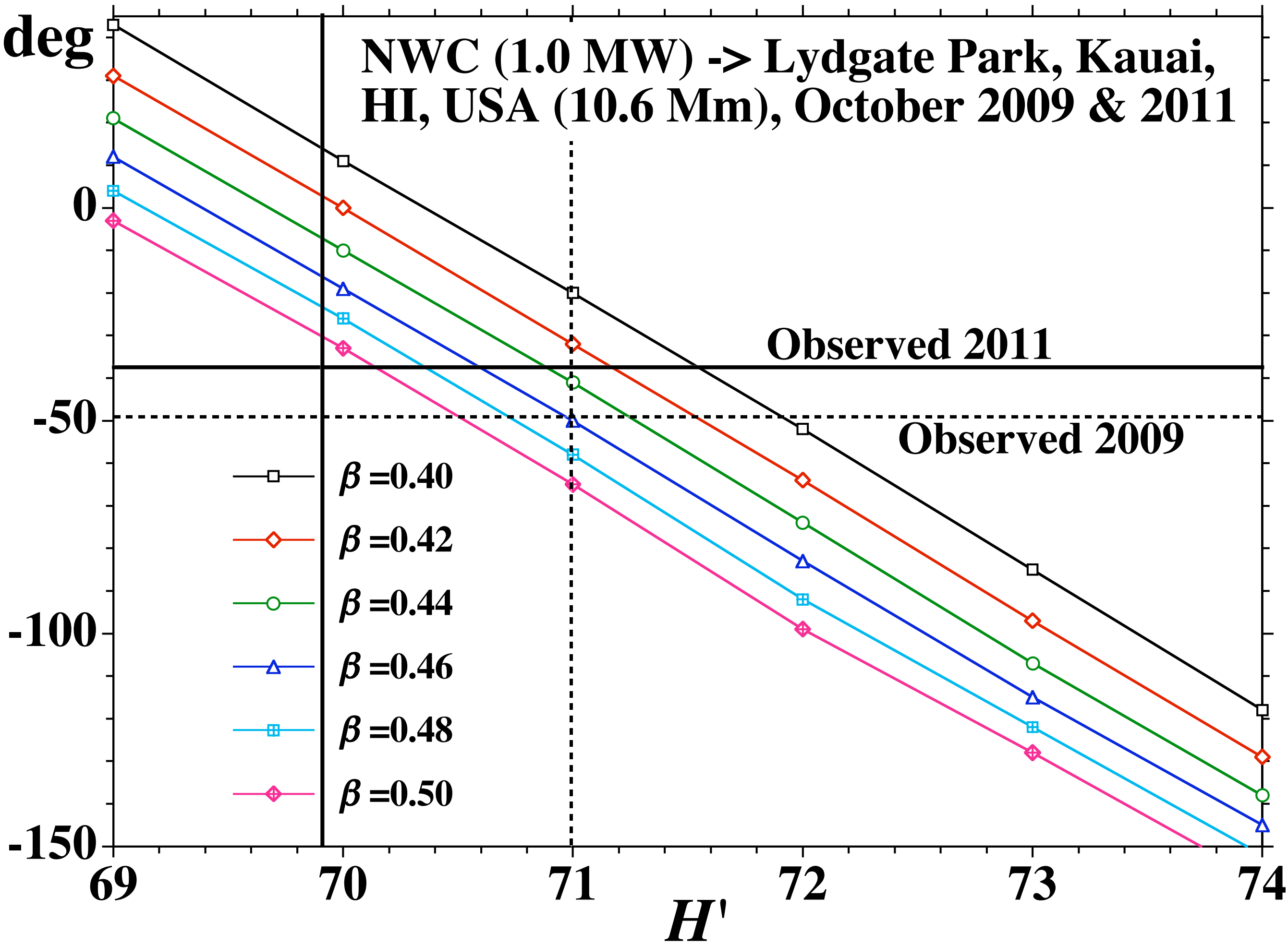
deg
NWC (1.0 MW) -> Lydgate Park, Kauai,
HI, USA (10.6 Mm), October 2009 & 2011
0
-50
-100
-150
Observed 2011
Observed 2009
β =0.40
β =0.42
β =0.44
β =0.46
β =0.48
β =0.50
69
70
71
72
73
74
H'

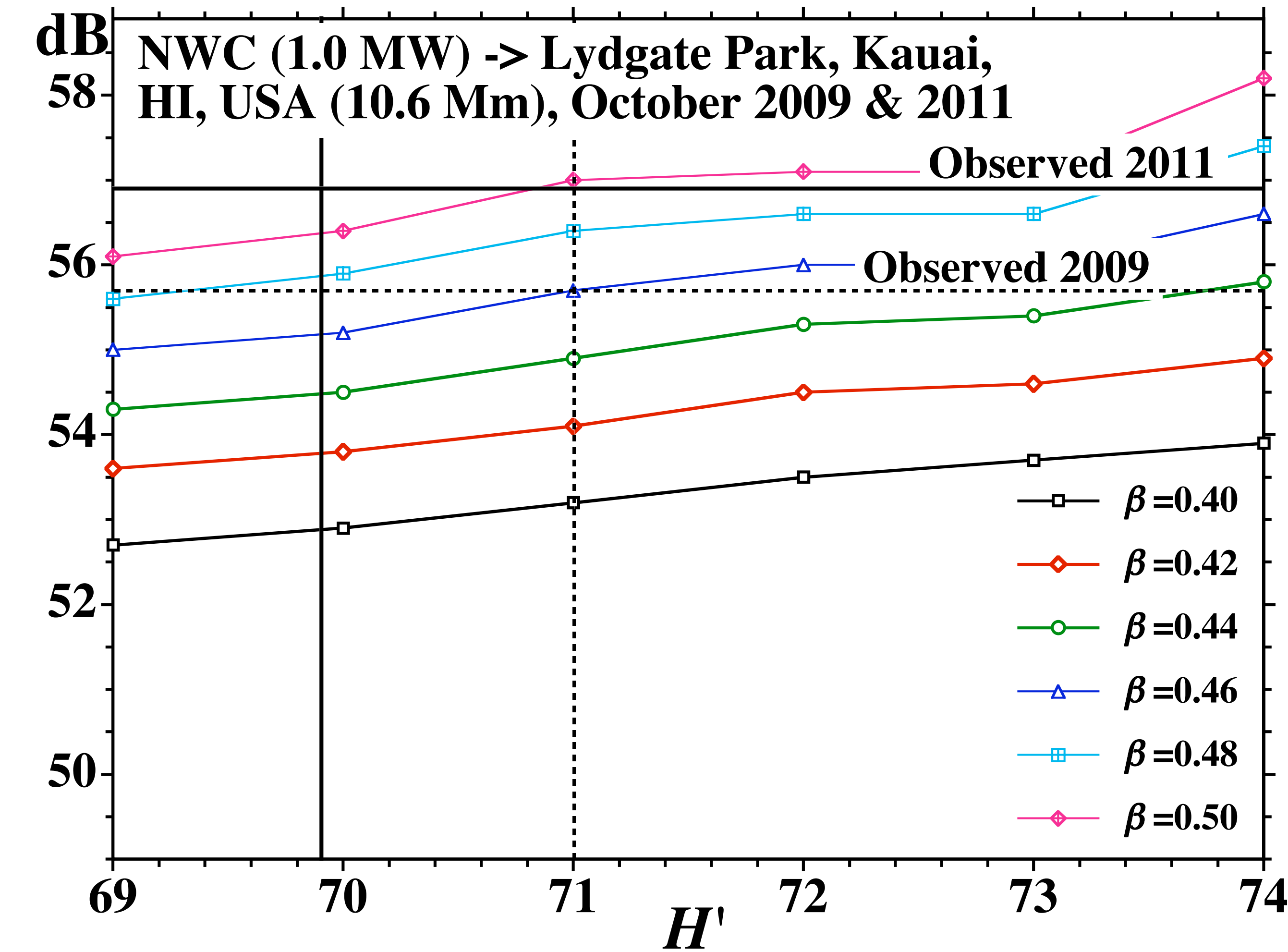
dB
NWC (1.0 MW) -> Lydgate Park, Kauai,
HI, USA (10.6 Mm), October 2009 & 2011
58
56
54
52
50
Observed 2011
Observed 2009
β =0.40
β =0.42
β =0.44
β =0.46
β =0.48
β =0.50
69
70
71
72
73
74
H'